Advances and Prospects of Digital Metrology

Jie Shen and David Yoon

University of Michigan-Dearborn, {shen | dhyoon}@umich.edu

ABSTRACT

In this paper, the authors first summarize recent advances in digital metrology at the Virtual Engineering Laboratory, the University of Michigan ì Dearborn. Different algorithms of surface denoising of laser scanning and computed tomography are then briefly discussed. Last, some challenges of digital metrology are provided for supporting high-precision digital manufacturing and industrial inspection.

1   INTRODUCTION

Metrology is the science of measurement. Digital metrology concerns the measurement via digital sensors. In this paper, we focus on the geometric information of physical objects and corresponding geometric sensors. With the proliferation of non-contact optical sensors such as laser scanners and X-ray computed tomography systems in recent years, fast measurement or reconstruction of physical objects has been practiced in many disciplines such as medicine, military, and engineering. Measurement errors due to various types of noise [1], however, still hinder the applications of these sensors or sensing systems in tolerance-sensitive metrology and reverse engineering [2-4].

Generally speaking, there are two major ways for eliminating the noise in three-dimensional (3D) surface/volume reconstruction or inspection. In the first way, a surface/volume mesh is constructed first [5, 6], and noise is removed next [7-10]; in the second way, the surface/volume reconstruction and denoising are mingled in a single step [11-16]. One advantage of the first way is that the separation of mesh/volume topology and denoising provides flexibility in determining mesh topology via user interaction in the presence of ambiguous data. It also facilitates experiments with different denoising algorithms. One benefit of the second way is an opportunity to optimize the reconstruction and denoising during one single coherent process.

The main objective of this paper is to summarize a series of recent studies on surface and volume denoising at the University of Michigan ì Dearborn. We will compare our schemes with typical existing approaches for both outliers and local noise at sharp edges and corners. Further, some research challenges are also discussed.

The remaining of this paper is organized as follows. In Section 2, we first introduce a novel spectral moving removal method for non-isolated outlier clusters. Then, a hybrid approach for denoising of objects with/without sharp features is described in Section 3, and a new local differentiation method is given in Section 4 for removing surface artifacts of three-dimensional volume data obtained from computed tomography. Finally, some challenges in digital metrology are given in Section 5.

2   MEASUREMENT OUTLIERS

Outliers are data points of measurement error, and have a significant distance from the true surface of the measured objects. Existing schemes [17-19] focus on discrete outliers, which can be synthetically generated by using a random number generator. Real-world sensing data are, however, in a more complex form: outlier cluster. Further, some outlier clusters are attached to the true data surface, as shown in Figure 1. This type of outliers poses a difficult challenge to existing algorithms of outlier removal.

(a) Over a continuous surface   (b) Around a sharp concave edge   (c) Around a sharp convex edge
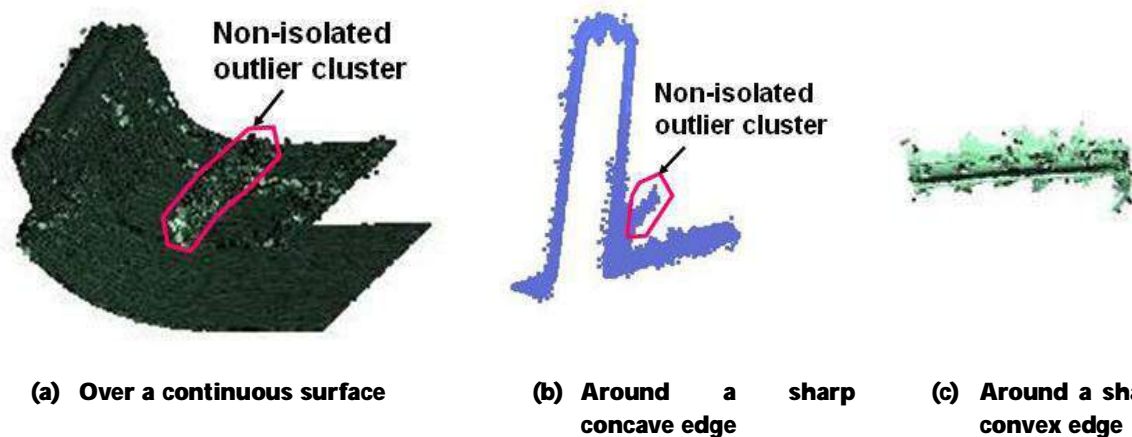
Fig. 1: Data clusters measured via a laser scanning system [20] (Non-isolated outlier cluster means a cluster that is attached to the true data surface).

The researchers in the Virtual Engineering Laboratory at the University of Michigan Ì Dearborn proposed a novel spectral moving removal (SMR) of data outliers [20]. This approach is effective on various types of measurement outliers, including non-isolated outlier clusters. The basic idea of SMR method is to utilize a minimum variance principle for designing an intrinsic metric for detecting outliers, to conduct a bi-means clustering for separating outliers from true data points, and to rely on a dual-sphere surface propagation for geometric coherence check.

The minimum variance principle (MVP) means that the measurement outliers could be classified by the variance within a neighborhood of each data point. The variance refers to the degree of point variation in a spatial neighborhood with respect to a specified central point. In a language of probability and statistics, it is a measure of statistical dispersion:

$$\sigma^2 = \sum_{i=1}^{n} p_i \left| \mathbf{x}_i - \boldsymbol{\mu} \right|_2^2 ,$$
(1)

Where σ^2 **is the variance, and** μ **is the mean vector of vectors** x_i $(i = 1, ..., n)$**.** p_i **is a probability mass function, and is assumed to be 1/n. The greater the variance is, the more probably the central point belongs to an outlier. The concept of MVP is different from traditional point-point distance in two main aspects:**

    (1) The variance in Equation (1) represents a summation, which transcends the right-hand side of the equation to a statistical dispersion, while traditional methods rely upon only simple calculation of point-point distance.

    (2) The variance calculation in our SMR approach is based upon spectral decomposition (i.e., eigenvalue decomposition). This results in an intrinsic metric, minimum variance, which is orientation-invariant for local point neighborhoods.

    Note that the variance computation is dependent upon the size of point neighborhoods. To obtain its size invariance, a normalized variance, $\hat{\sigma}^2$**, was defined as [20]**

$$\hat{\sigma}^2 = \begin{cases} \dfrac{\sigma^2 - \sigma_{\min}^2}{\sigma_{\max}^2 - \sigma_{\min}^2}, & \sigma_{\max}^2 > \sigma_{\min}^2 \\ 1, & \sigma_{\max}^2 = \sigma_{\min}^2 \end{cases}, \tag{2}$$

where $\sigma_{\min}^2$ **and** $\sigma_{\max}^2$ **are the smallest and greatest variances among all local point neighborhoods.**

    To implement the concept of minimum variance principle, a covariance matrix is used in each point neighborhood:

$$\mathbf{C} = \mathrm{E}\left[(\mathbf{x} - \boldsymbol{\mu}) \otimes (\mathbf{x} - \boldsymbol{\mu})\right] = \mathrm{E}\left[(\mathbf{x} - \boldsymbol{\mu}) \cdot (\mathbf{x} - \boldsymbol{\mu})^*\right] = \frac{1}{n}(\mathbf{x} - \boldsymbol{\mu}) \cdot (\mathbf{x} - \boldsymbol{\mu})^*, \tag{3}$$

where $\mathbf{x}$ **and** $\boldsymbol{\mu}$ **represent data point and its mean vector, respectively.** E **is an expected value operator, and** $\otimes$ **refers to an outer production operator.** * **is a conjugate transpose operator that is equivalent to a regular transpose operator, because** $\mathbf{x} - \boldsymbol{\mu}$ **contains only real entries.**

    The eigenvalues of the matrix in Equation (3) are sample variances along principal directions (i.e., the directions corresponding to eigenvectors). Our *minimum variance principle* **is then transformed to a premise that the greater the smallest sample variance** λ_3 **is, the more probably the local point cloud belongs to outliers. This assumption is valid for smooth surfaces except sharp edges or corners. We rely on a specially-designed surface propagation scheme to avoid applying minimum variance principle at sharp edges and corners. From the standpoint of spectral analysis, the smallest eigenvalue can be named as minimum spectral radius, which signifies the least statistic dispersion at each point neighborhood. Compared with the traditional clustering of global spectral graph [18], the implementation of local covariance matrix in our approach is involved with only local operations, and therefore is much more computationally efficient.**

    To separate the outliers from true data points, a special type of K-means clustering, Bi-means clustering, is utilized on the basis of Lloyd's algorithm [21]. For geometric coherence check and for handling the sharp features, an automatic surface propagation is adopted. The surface propagation is automatically started from a finite number, *m* **(***m* **is much smaller than** *n***), of seeding points, which are selected by randomly sampling points and selecting those with low variance and high point density. We use a kd-tree data structure of measurement points and moving least-square fitting of local quadratic surface patches for supporting the surface propagation.**

    Figure 2 demonstrates the effectiveness of our moving spectral removal of outlier clusters against existing methods. To the best knowledge of the authors in this paper, so far our method is the only one, which is effective on eliminating non-isolated outlier clusters.

(a) Original measured model (b) Outlier removal via our method (c) Outlier removal via the well-known Weyrich method [19]
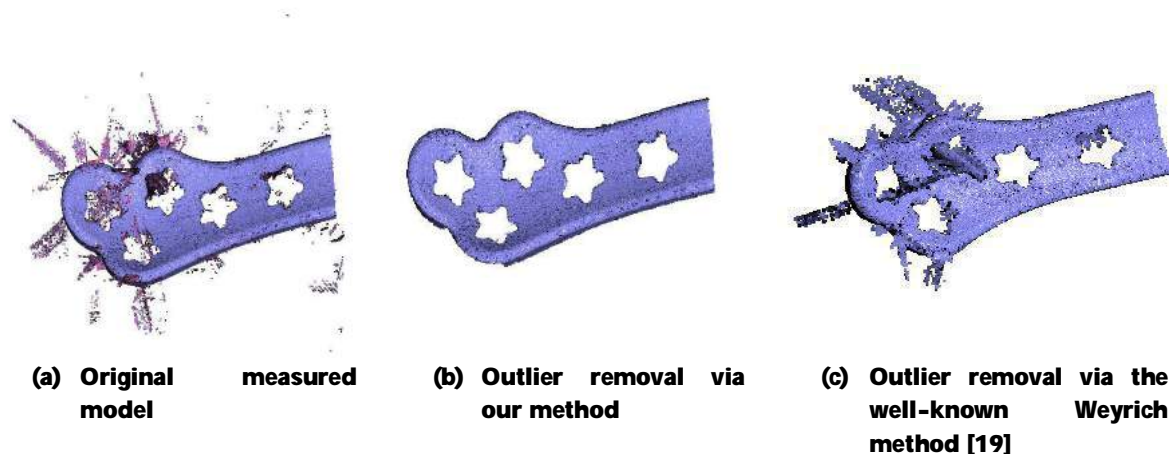
Fig. 2: Digital model of a mechanical part measured by a laser scanner [20].

3   LOCAL NOISE AT SHARP EDGES/CORNERS

One very good algorithm in removing the measurement noise at sharp edges or corners is median filter or its variants [10, 22]. The median filter can, however, not effectively eliminate some local small-magnitude noise at sharp edges or corners [23]. Bilateral filter or anisotropic diffusion is another group of well-studied algorithms that can be used to handle sharp edge or corner problems [8, 9, 24–34]. Most of these approaches were developed for the applications in computer graphics in which visual effect is their major concern. Unfortunately, the bilateral schemes in [26, 33] do not guarantee the accurate removal of noise near sharp edges or corners in some special cases. This deficiency is not desirable for high-precision industrial inspection or modeling. Piecewise least-squares fitting is yet one more approach to deal with the sharp edges and corners. How to determine the intersection between different surface patches is still an open question. There is very few published literature for reporting a quantitative comparison among different algorithms in terms of denoising accuracy.

For a better convergence and denoising accuracy, we proposed a hybrid denoising approach for handling arbitrary objects with/without sharp features [35]. The basic rational of our approach is that we should use two different algorithms respectively for the continuous and discontinuous parts of object surfaces, because the geometric property of these two parts is not the same at all. The outline of the approach is as follows:

Step 1: Feature-Preserving Pre-Smoothing

A pre-smoothing step is crucial for partitioning of an object into geometrically continuous and discontinuous parts. Since the scanned data contain a certain amount of noise, the noise would pose a serious challenge to any surface partitioning algorithm. If we use a regular smoothing algorithm to pre-process the digital data as in [8, 9, 33], the algorithm would smooth out some sharp features. This is not desirable and would affect the quality of an overall approach.

Our novel idea is to adopt a feature-preserving pre-smoothing (median filter) that does not require any threshold and implicitly retains the sharp features. The salient feature of this pre-smoothing algorithm is that the median fileter does not require any partitioning information of geometrically continuous and discontinuous regions.

Step 2: Surface Partitioning

We use G^1 geometric discontinuity and curvature threshold as an indicator for surface partitioning of feature and non-feature regions. *Feature regions* are defined as the areas in which either sharp edges or high curvatures exist, and the remaining parts are called the *non-feature regions*. A simple threshold or an adaptive threshold can be applied in the partitioning. There is a vast amount of literature related to different approaches for estimating discrete curvatures [30, 36–40]. But, very few reports are available for the comparison among these schemes with respect to accuracy, convergence and computational efficiency. In reference [35], we proposed an accurate estimation of discrete nodal curvature with a mathematically-proven convergence.

Step 3: Smoothing Feature Region

In the feature regions, we apply a median filter for the second time. Compared with anisotropic diffusion algorithms, its main advantage is no need for the information on the directions of principal curvatures. Such directions are invalid at singular points (e.g., an apex of a cone). The median filter also avoids some pitfalls of bilateral filters at sharp edges, as explained in [35].

Step 4: Smoothing Non-Feature Region

We design a second-order predictor as an accurate indicator for guiding a surface smoothing process in non-feature regions. It is essentially a modified version of moving least-squares fitting. The main benefit of the proposed second-order predictor is a better accuracy and convergence with curved surfaces than the first-order predictors, mean-curvature flow and Gaussian predictors in existing algorithms. The key components of our second-order predictor include a) a robust least-squares fitting procedure to fit each surface neighborhood with a local quadric patch, and b) a fast procedure to determine our second-order predictor.

Step 5: Hybrid Smoothing

By applying our second-order predictor in non-feature regions and utilizing the median filter in feature regions, we come up with a hybrid approach that performs consistently better than existing algorithms with different types of noisy data models in terms of convergence and denoising accuracy.

Figure 3 shows a quantitative comparison between our hybrid scheme and several existing methods in terms of a geometric error metric. The smaller this metric is, the higher the denoising accuracy becomes. The figure indicates that our approach is the best among seven different algorithms.

(a) Noisy data   (b) Denoised data   (c) Denoising accuracy
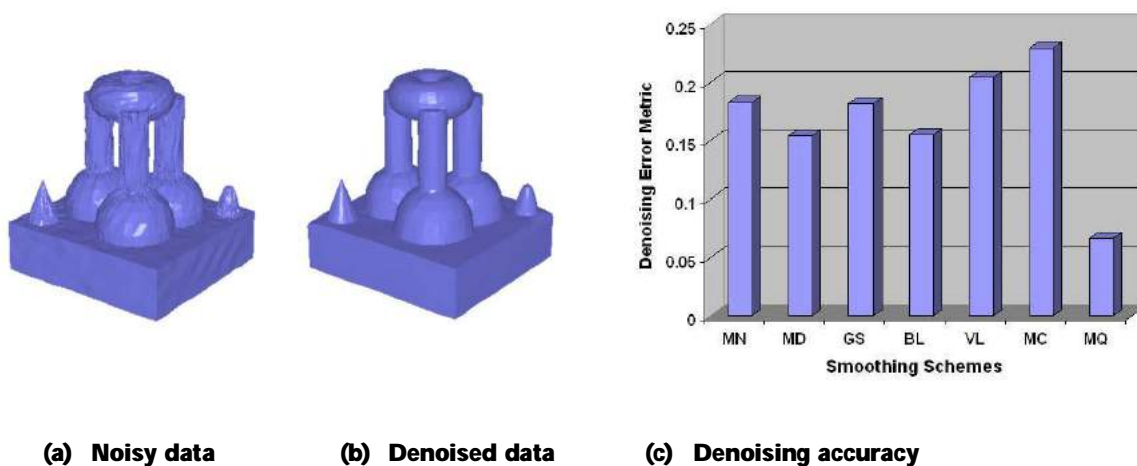
Fig. 3: Comparison between our hybrid scheme and existing smoothing methods [35] (MN–mean filter; MD–median filter; GS–Gaussian filter; BL–bilateral filter; VL–volumetric Laplacian; MC–mean curvature flow; MQ–our hybrid scheme).

4 VOLUME DENOISING OF TOMOGRAPHY DATA

X–ray computed tomography (CT) is a digital measurement technique to generate a three–dimensional image and geometric object from a series of two–dimensional X–ray images. Because of its rapid development in recent years, it has been applied in many engineering fields for inspection and modeling. Nano CT and micro–focus CT extend this technique into microscale and nanoscale world, in which many scientific and engineering questions still need to be answered. In this section, we focus on the digital inspection and modeling of internal defects of engineering material specimens. One issue of material specimens is their surface roughness, which complicates the defect detection of computed tomography data. In our recent study [41], we proposed a novel *local differentiation* algorithm to remove the surface artifacts caused by surface roughness in the defect detection of material specimens.

The surface of material specimens may not be well polished, leading to a high surface roughness. This will influence the surface/volume recognition of material defects. The peaks and valleys on material surface are often recognized as defects by using traditional scan line algorithm. For metal alloy specimens with a low defect volume fraction (i.e., 0.05%), the prediction error of defect volume fraction could reach 100% if we use the traditional scan line approach. Therefore, it is important for us to come up with a new scheme to alleviate the impact of surface roughness on the accurate detection of defect distribution.

The basic idea of our approach is to utilize the information of voxel state change in a local neighborhood. The state herein refers to different types of voxels (background, material and defect), and the state change means a transition from one voxel type to another. The goal of our method is to provide different labels to the boundaries of material defects and surface artifacts due to surface roughness, as illustrated in Figure 4. It demonstrates that an internal defect is surrounded by material elements (m) and a surface opening has boundary elements (b) as neighbors.
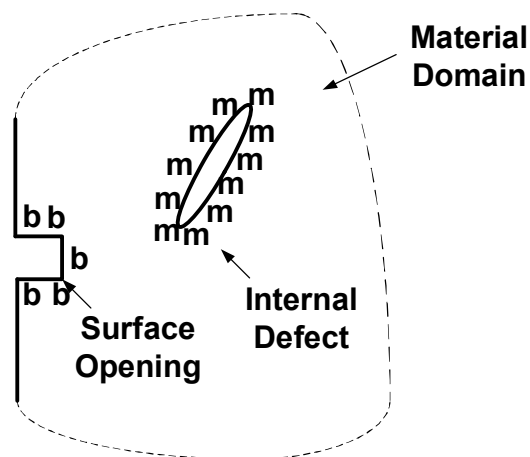
Fig. 4: Labeling of an internal defect and a surface opening in local differentiation method.

In the implementation of our local differentiation method, it is first necessary to segment the material from everything else. If there is uniform illumination, a simple histogram threshold is used. Otherwise, an adaptive threshold should be used. For every voxel, if the voxel is within the given threshold, that voxel is labeled as material ("m"); otherwise it is temporarily labeled as a defect ("o"). A three-layer iteration is used. The first loop is to traverse along one of the three coordinate axes, and the second loop is to move along one of the remaining two axes. In the third loop, a scan-line movement is conducted twice in two opposite directions of the coordinate axis that is not used in the first two loops. Overall, there are twelve loops in this three-layer iteration. In each loop, our algorithm changes the label of voxels to BACKGROUND until a voxel that has been labeled MATERIAL is reached; once that happens, the label is changed from MATERIAL to BOUNDARY; if there is a neighboring MATERIAL voxel on a previous scan line, change it to BOUNDARY. At the end of our algorithm, material voxels are labeled as either MATERIAL or BOUNDARY; internal defect is labeled as DEFECT, and background space is marked as BACKGROUND.

Figure 5 illustrates the two loops in our local differentiation method. Symbol "o" represents an outsider element, while "m" refers to a material element. During each scan, some elements become "b", which denotes a boundary element. SEM (Scanning Electron Microscopy) material tests indicate that our local differentiation method is about 64% better than the traditional scan line method in terms of accuracy for predicting material defect fraction.
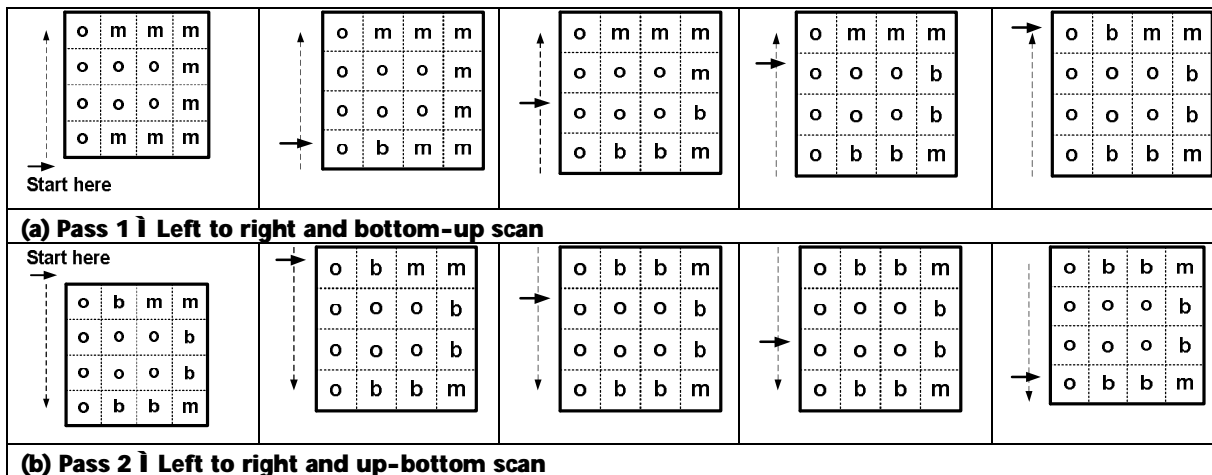
Fig. 5: Two typical passes of the local differentiation [41].

5 RESEARCH CHALLENGES

Although a considerable amount of effort has been devoted in the past, there are still some open issues in the area of digital metrology. To date, there is no geometric sensor that can automatically measure the geometric discontinuity at high precision and robustness. Piecewise fitting of digital data – a brute force approach – faces a detrimental chicken-and-egg problem, in which the correct surface partition (chicken) relies on the information of true surface normal (egg), but the surface normal needs to be accurately estimated from the information of surface partition. This problem becomes evident at discontinuity where the surface normal is ambiguous and a feature line is shared by two surface patches. discontinuity means no continuity in the direction of surface normal in a loose sense, and is the most prevailing geometric discontinuity among manufactured parts in various industries.

Further on the laser scanning techniques, the multiple reflections on shinny metallic surfaces of mechanical parts and the scattering of light inside a translucid material (Figure 6) pose a more serious threat to geometric sensing (especially sensors based on triangulation principle). In such a case, the surface needs to be sprayed with a thin-layer optically-diffusive coating or a digital filter algorithm is applied to preprocess laser stripe images.

(a) Interaction between a laser beam and a translucid surface

(b) Visual effect on a translucid surface

(c) Digital measurement points on a translucid surface
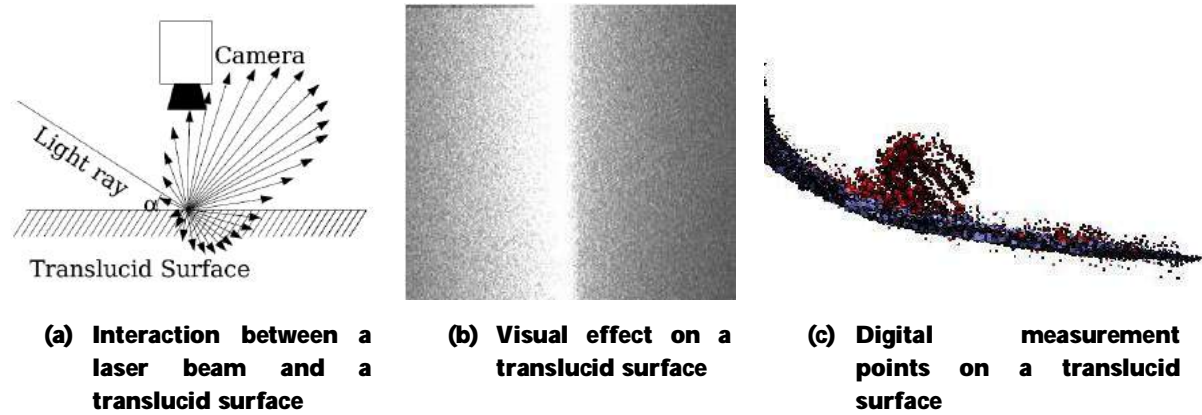
Fig. 6: Laser scanning problem with translucid surfaces [42].

In the area of computed tomography, inspection and modeling of polymer foams face two grand challenges:

(a) The cellular walls of some foams are very thin (about 10 -20 micrometers);
(b) Polymer is a light-weight material that has very low attenuation to X-ray penetration.

As a result, the intensity contrast of X-ray images is not high enough, as shown in Figure 7(b), in which background space is in black color and the foam wall in grey-white color. Note that this figure is not an exact cross section. Instead, it is an overlap of the current cross section and the cellular structures behind the cross section. Even if a sophisticated adaptive thresholding algorithm is used, the segmentation result (Figure 7(c)) is still unsatisfactory. In Figure 7(c), the cellular walls are in black color and the air is in white color. This poor result has an immediate impact on the accurate surface reconstruction of the cellular structures and subsequent finite element analysis.

(a) Polymer foam specimen

(b) X-ray image of part of the specimen in a finer scale (one pixel=10 microns)

(c) Two-dimensional segmentation of part of the specimen in a finer scale (one pixel = 10 microns)
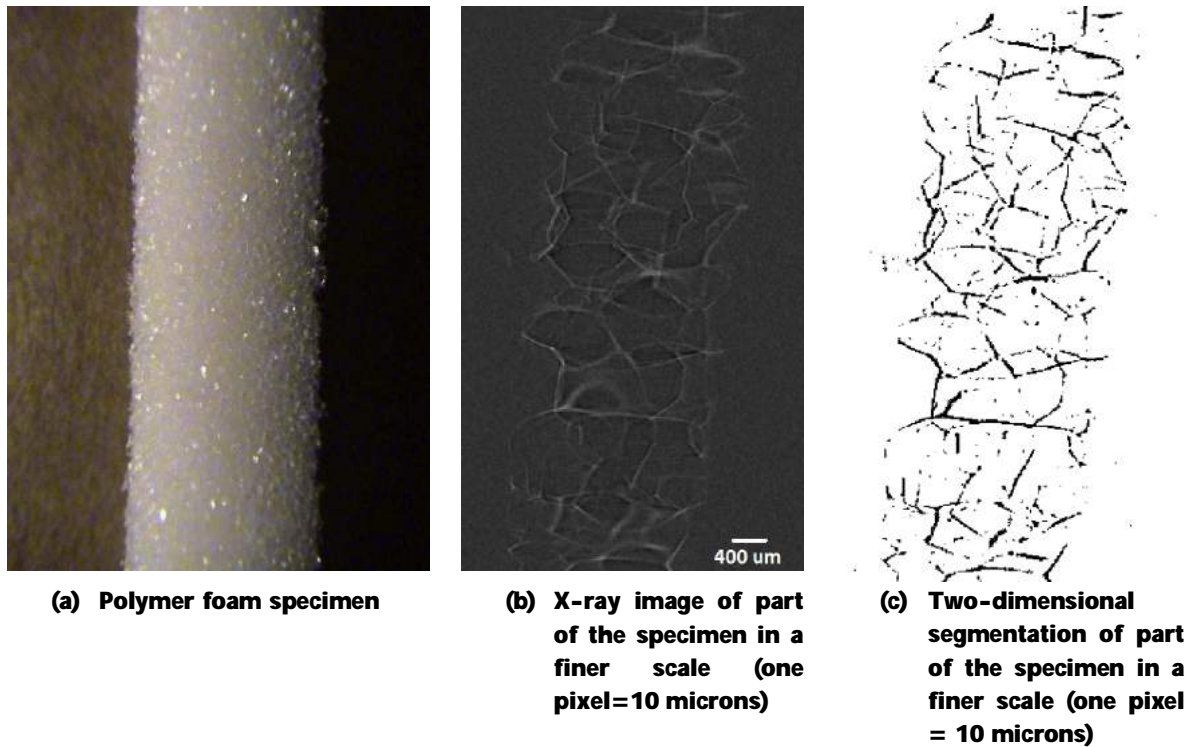
Fig. 7: Reconstruction challenge with polymer foam specimens.

6   ACKNOWLEGEMENT

REFERENCES

[1]   Dorsch, R. G.; Hausler, G.; Herrmann, J. M.: Laser triangulation: fundamental uncertainty in distance measurement, Applied Optics, 33(7), 1994, 1306–1314.

[2]   Klinger, P.; Veit, K.; Hausler, G.; Karbacher, S.; Laboureux, X.: Optical 3D sensors for real applications – potentials and limits, Proceedings of the 8th International Rendez–vous for 3D Digitisation and Modeling Professionals, 2003, 1–5 (pdf file available at http://www.optik.uni-erlangen.de/osmin/research/papers.php).

[3]   Bernardini, F.; Bajaj, C. L.; Chen, J.; Schikore, D. R.: Automatic reconstruction of 3D CAD models from digital scans, International Journal of Computational Geometry & Applications, 9(4 & 5), 1999, 327–369.

[4]   Varady, T.; Martin, R. R.; Cox, J.: Reverse engineering of geometric models – an introduction, Computer Aided Design, 29(4), 1997, 255–269.

[5]   Curless, B.; Levoy, M.: A volumetric method for building complex models from range images., Proceedings of ACM SIGGRAPH, 1996, 303–312.

[6]   Turk, G.; Levoy, M.: Zippered polygon meshes from range images, 1994, 311–318.

[7]   Belyaev, A.; Ohtake, Y.: A comparison of mesh smoothing methods, Israel–Korea Bi-National Conference on Geometric Modeling and Computer Graphics, 2003, 83–87.

[8]   Clarenz, U.; Diewald, U.; Rumpf, M.: Anisotropic geometric diffusion in surface processing, Proceedings of IEEE Visualization, 2000, 397–405.

[9]   Desbrun, M.; Meyer, M.; Schroder, P.; Barr, A. H.: Anisotropic feature-preserving denoising of height fields and bivariate data, Graphics Interface, 2000, 145–152.

[10]   Shen, Y.; Barner, K. E.: Fuzzy vector median-based surface smoothing, IEEE Transactions on Visualization and Computer Graphics, 10(3), 2004, 266–277.

[11]   Carr, J. C.; Beatson, R. K.; Cherrie, J. B.; Mitchell, T. J.; Fright, W. R.; McCallum, B. C.; Evans, T. R.: Reconstruction and representation of 3d objects with radial basis functions, Proceedings of ACM SIGGRAPH, 2001, 67–76.

[12]   Morse, B. S.; Yoo, T. S.; Rheingans, P.; Chen, D. T.; Subramanian, K. R.: Interpolating implicit surfaces from scattered surface data using compactly supported radial basis functions, Proceedings of International Conference on Shape Modeling and Applications '01, 2001, 89–98., IEEE Computer Society Press.

[13]   Dinh, H. Q.; Turk, G.; Slabaugh, G.: Reconstructing surfaces using anisotropic basis functions, Proceedings of ICCV 2001, 2001, 606–613.

[14]   Fleishman, S.; Cohen-Or, D.; Silva, C.: Robust moving least-squares fitting with sharp features, ACM Transactions on Graphics., 24(3), 2005, 544–552.

[15]   Ohtake, Y.; Belyaev, A.; Seidel, H.: Multi-level partition of unity implicits, 2003, 27–31.

[16]   Dey, T. K.; Sun, J.: An adaptive MLS surface for reconstruction with guarantees, Eurographics Symposium on Geometry Processing (2005), 2005, Desbrun, M. and Pottmann, H.

[17]   Xie, H.; McDonnell, K. T.; Qin, H.: Surface reconstruction of noisy and defective data sets, IEEE Visualization 2004, 2004, 259–266.

[18]   Kolluri, R.; Shewchuk, J. R.; O'Brien, J. F.: Spectral surface reconstruction from noisy point clouds, Symposium on Geometry Processing, 2004, 11–21.

[19]   Weyrich, T.; Pauly, M.; Keiser, R.; Heinzle, S.; Scandella, S.; Gross, M.: Post-processing of scanned 3D surface data, Proceedings of Eurographics Symposium on Point-Based Graphics, 2004, 85–94.

[20]   Shen, J.; Yoon, D.; Shehu, D.; Chang, S. Y.: Spectral moving removal of non-isolated surface outlier clusters, Computer-Aided Design, 41(4), 2009, 256–267.

[21]   Lloyd, S. P.: Least squares quantization in PCM, IEEE Transactions on Information Theory, 28(2), 1982, 129–137.

[22]   Yagou, H.; Ohtake, Y.; Belyaev, A.: Mesh Smoothing via Mean and Median Filtering Applied to Face Normals, Geometric Modeling and Processing 2002, 2002, 124–131.

[23]   Shen, J.; Yoon, D.; Shou, H.; Zhao, D.; Liu, S.: Denoising two-dimensional geometric continuities, (submitted for publication), 2006,

[24]   Perona, P.; Malik, J.: Scale-space and edge detection using anisotropic diffusion, IEEE Transactions on Pattern Analysis and Machine Intelligence, 12(7), 1990, 629–639.

[25]   Tomasi, C.; Manduchi, R.: Bilateral filtering for gray and color images, Proceedings of IEEE ICCV, 1998, 836–846.

[26]   Fleishman, S.; Drori, I.; Cohen-Or, D.: Bilateral mesh denoising, Proceedings of the 30th Annual Conference on Computer Graphics and Interactive Techniques, 2003, 950–953.

[27]   Choudhury, P.; Tumblin, J.: The trilateral filter for high contrast images and meshes, Christensen, Per. H. and Cohen, D. Proceedings of the Eurographics Symposium on Rendering, 2003, 186–196.

[28]   Ohtake, Y.; Belyaev, A.; Seidel, H.: Mesh smoothing by adaptive and anisotropic Gaussian filter, Vision, Modeling, and Visualization 2002, 2002, 203–210.

[29]   Bajaj, C.; Xu, G.: Anisotropic diffusion of subdivision surfaces and functions on surfaces, ACM Transactions on Graphics, 22(1), 2003, 4–32.

[30] Meyer, M.; Desbrun, M.; Schroder, P.; Barr, A. H.: Discrete differential-geometry operators for triangulated 2-manifolds, In Visualization and Mathematics III. pp. 35-57, Springer-Verlag, Heidelberg, 2003.

[31] Tasdizen, T.; Whitaker, R. T.; Burchard, P.; Osher, S.: Anisotropic geometric diffusion in surface processing, IEEE Visualization 2002, 2002, 125-132.

[32] Zhang, H.; Fiume, E. L.: Mesh smoothing with shape or feature preservation, In Advanced in modeling, animation, and rendering. (Ed. J. Vince and R. Earnshaw) pp. 167-182, Springer, 2002.

[33] Jones, T. R.; Durant, F.; Desbrun, M.: Non-iterative, feature-preserving mesh smoothing, Proceedings of the 30th Annual Conference on Computer Graphics and Interactive Techniques, 2003, 943-949.

[34] Hildebrandt, K.; Polthier, K.: Anisotropic filtering of non-linear surface features, Computer Graphics Forum, 23(3), 2004, 391-400.

[35] Shen, J.; Maxim, B.; Akingbehin, K.: Accurate Correction of Surface Noises of Polygonal Meshes, International Journal for Numerical Methods in Engineering, 64(12), 2005, 1678-1698.

[36] Alboul, L.: Optimising triangulated polyhedral surfaces with self-intersections, Proceedings of the 10th IMA International Conference,2768, 2003, 48-72.

[37] Calladine, C.: Gaussian curvature and shell structure, In. pp. 179-196, Oxford: Clarendon Press, 1986.

[38] Kobbelt, L.: Discrete fairing and variational subdivision for free-form surface design, The Visual Computer, 16(3/4), 2000, 142-158.

[39] Krsek, P.; Lukacs, G.; Martin, R. R.: Algorithms for computing curvatures from range data, Cripps, R. J. Proceedings of the Eighth IMA Conference on the Mathematics of Surfaces, 1998, 1-16.

[40] Mangan, A. P.; Whitaker, R. T.: Partitioning 3D surface meshes using watershed segmentation, IEEE Transactions on Visulization and Computer Graphics, 5(4), 1999, 308-321.

[41] Shen, J.; Diego, V.; Yoon, D.: Removal of surface artifacts of material volume data with defects, Murgante, B., Gervasi, O., Iglesias, A., Taniar, D., and Apduhan, B. O. Computational Science and Its Applications – ICCSA 2011, 2011, 624-634., Springer.

[42] Forest, J.; Salvi, J.; Cabruja, E.; Pous, C.: Laser stripe peak detector for 3D scanners. A FIR filter approach, Proceedings of the 17th International Conference on Pattern Recognition, 3, 2004, 646-649.